

Frobenius-Perron Resonances for Maps with a Mixed Phase Space

Joachim Weber¹, Fritz Haake¹, and Petr Šeba²

¹ *Fachbereich Physik, Universität-GH Essen, 45117 Essen, Germany*

² *Institute of Physics, Czech Academy of Sciences, Prague, Czech Republic*

(Date: October 28, 2018)

Resonances of the time evolution (Frobenius-Perron) operator \mathcal{P} for phase space densities have recently been shown to play a key role for the interrelations of classical, semiclassical and quantum dynamics. Efficient methods to determine resonances are thus in demand, in particular for Hamiltonian systems displaying a mix of chaotic and regular behavior. We present a powerful method based on truncating \mathcal{P} to a finite matrix which not only allows to identify resonances but also the associated phase space structures. It is demonstrated to work well for a prototypical dynamical system.

PACS numbers: 05.45.-a, 05.45.Mt, 05.20.-y

Effectively irreversible behavior of classical Hamiltonian systems can be elucidated by studying the phase space density and its propagator, the Frobenius-Perron operator \mathcal{P} . Due to Liouville's theorem \mathcal{P} can be represented by an infinite unitary matrix whose spectrum lies on the unit circle in the complex plane. Nevertheless, means and correlation functions of observables can relax (see figure 1c) with damping factors known as (Ruelle-Pollicott) resonances [1–4] of \mathcal{P} . These resonances have recently attracted attention, e.g. in a superanalytic approach to universal fluctuations in quantum (quasi-) energy spectra which originated from the physics of disordered systems. In that approach the Frobenius-Perron resonances constitute a link between classical and quantum chaos [5,6]. There is even a recent experiment where quantum fingerprints of Ruelle-Pollicott resonances are identified [7]. To further clarify the interrelations between classical, semiclassical, and quantum behavior, a practical scheme to actually determine classical resonances is called for which is free of restrictions of previous investigations, like hyperbolicity, one-dimensional (quasi-) phase space or isolation of the phase-space regions causing intermittency.

Our thus motivated quantitative investigations into Hamiltonian systems with mixed phase space, a still largely unexplored area of great interest and promise, lead us to the discrete unimodular Frobenius-Perron eigenvalues (with eigenfunctions localized in islands of regular motion around elliptic periodic orbits, see figure 1a) and to resonances, smaller than unity in modulus (with eigenfunctions localized on the unstable manifolds of hyperbolic periodic orbits, see figure 2a-c). Both the discrete spectrum and the resonances are determined by diagonalizing truncated Frobenius-Perron matrices $\mathcal{P}^{(N)}$

and studying the cut-off dependence of its eigenvalues. Using the information about eigenfunctions, we then reproduce resonances by the so-called cycle expansion of periodic-orbit theory and furthermore through decay rates of correlation functions. We should add that similarly motivated but technically different (not involving eigenfunctions and employing external noise) efforts to determine resonances can be found in Refs. [8–10].

As a prototypical dynamical system we have employed the kicked top, i.e. a periodically kicked angular momentum $\vec{J} = (j \sin \theta \cos \varphi, j \sin \theta \sin \varphi, j \cos \theta)$ of conserved length j whose phase space is the sphere $\vec{J}^2/j^2 = 1$; we confront a single degree of freedom with the “azimuthal” angle ϕ as the coordinate and the cosine of the “polar” angle θ the conjugate momentum. The dynamics is specified as a stroboscopic area preserving map M on phase space. It consists of rotations $R_z(\beta_z), R_y(\beta_y)$ about the y - and z -axes and a “torsion”, i.e. a nonlinear rotation $R_z(\tau \cos \theta)$ about the z -axis which changes φ by $\tau \cos \theta$,

$$M = R_z(\tau \cos \theta) R_z(\beta_z) R_y(\beta_y). \quad (1)$$

The equivalent map of the phase space density ρ is brought about by the Frobenius-Perron operator \mathcal{P} ,

$$\mathcal{P}\rho(\cos \theta, \varphi) = \rho(M^{-1}(\cos \theta, \varphi)). \quad (2)$$

We keep $\beta_z = \beta_y = 1$ fixed and vary the torsion constant τ , starting with the integrable case $\tau = 0$. Increasing values of τ bring about more and more chaos until for $\tau > 10$ elliptic islands have become so small that they are difficult to detect. We shall focus on $\tau = 4$ (roughly 90% of the phase space dominated by chaos) and $\tau = 10$ (more than 99% chaos).

A Hilbert space of phase space functions on the sphere is spanned by the spherical harmonics $Y_{lm}(\theta, \varphi)$ with $l = 0, 1, 2, \dots$ and $|m| \leq l$. These functions are ordered with respect to phase space resolution by the index l : if all Y_{lm} with $0 \leq l \leq l_{max}$ are admitted phase space structures of area roughly $4\pi/(l_{max} + 1)^2$ can be resolved. If we so truncate the infinite Frobenius-Perron matrix $\mathcal{P}_{lm, l'm'}$, we (i) destroy unitarity, (ii) restrict the spectrum to $N = (l_{max} + 1)^2$ discrete eigenvalues whose moduli cannot exceed unity, and (iii) renounce the resolution of phase space structures of linear dimension below $\sqrt{4\pi}/(l_{max} + 1)$. Upon diagonalizing the truncated $N \times N$ matrix $\mathcal{P}^{(N)}$ and increasing N we find the “newly born” eigenvalues close to the origin while the “older” ones move about in the complex plane. “Very old” ones

eventually settle for good. If the classical dynamics is integrable ($\tau = 0$ or $\beta_y = 0$), the asymptotic large- N loci are back to the unit circle, where the full \mathcal{P} has its spectrum. But not so for a mixed phase space: while some eigenvalues of $\mathcal{P}^{(N)}$ “freeze” with unit moduli, others come to rest inside the unit circle as $N \rightarrow \infty$. Table I illustrates how non-unimodular eigenvalues found for the kicked top with $\tau = 10$ at $l_{max} = 40$ remain in their positions as l_{max} is increased to $l_{max} = 50, 60$ and 70 .

We could pass over such findings and speak of the danger of tampering with infinity, were there not good reasons for and a physical interpretation of the existence of such stable non-unimodular eigenvalues.

The following qualitative argument suggests the persistence of non-unimodular eigenvalues as $N \rightarrow \infty$ for non-integrable dynamics. In contrast to regular motion, chaos brings about a hierarchy of phase space structures which extends without end to ever finer scales. A truncated Frobenius-Perron operator $\mathcal{P}^{(N)}$ must reflect the flow of probability towards the unresolved scales as a loss, however large the cut-off N may be chosen.

Arguments from perturbation theory [13,14] indicate that any non-unitary approximation to a unitary operator with continuous spectrum has some eigenvalues in positions near (non-unimodular) resonances of the unitary operator, i.e. poles of the resolvent in a higher Riemannian sheet. The perturbation series for such an eigenvalue does not converge but produces, with increasing order, a sequence of points concentrated in the neighborhood of the respective resonance. It is intuitive to interpret the freezing of non-unimodular eigenvalues (which need not be a strict convergence) as analogous to the “spectral concentration” known from perturbation theory.

To find further evidence for our interpretation of frozen eigenvalues as resonances we have looked at the eigenfunctions of $\mathcal{P}^{(N)}$, with the following salient results. Eigenvalues freezing with unit moduli have eigenfunctions located on elliptic islands of regular motion surrounding elliptic periodic orbits in phase space. Such islands are bounded by invariant tori which form impenetrable barriers in phase space. We can thus expect the function constant inside the elliptic islands around a p -periodic orbit and zero outside to be an eigenfunction of \mathcal{P} with eigenvalue unity. Similarly reasoning we expect, for $p > 1$, the p th roots of unity to arise as eigenvalues as well; their eigenfunctions should have constant moduli and be invariant under \mathcal{P}^p . For the kicked top with $\tau = 4$ and $l_{max} = 60$ an eigenfunction with the eigenvalue 0.9993, i. e. almost at unity, is shown in figure 1a. It is localized on the three islands around an elliptic orbit of period three (see figure 1b) and does have the two expected partners. We have indeed found frozen eigenvalues near the p -th roots of unity and their eigenfunctions localized near elliptic period- p orbits for p up to 6; without much further effort such signatures of higher periods could be identified.

Now on to the eigenvalues freezing with moduli smaller than unity. Once such freezing has been observed the corresponding eigenfunction has approached its final shape on the resolved phase space scales. The eigenfunctions are sharply localized around unstable manifolds of hyperbolic periodic orbits, ones with low periods at first since these are easiest to resolve; but with growing l_{max} more complex orbits of higher periods appear in the “support” of eigenfunctions. Even though all periodic orbits contributing to the structure of an eigenfunction have similar stability coefficients and even though the latter do describe the rate of mutual departure of neighboring trajectories it would be too naive to simply identify resonances with stability coefficients; we shall rather have to resort to cycle expansions further below.

Just as for the eigenvalues there is no strict convergence of the eigenfunctions. With increasing resolution new structures on finer scales become visible, in correspondence with the infinitely convoluted shape of the unstable manifolds (see figure 2a-b). Since no finite approximation $\mathcal{P}^{(N)}$ accounts for arbitrarily fine structures one encounters the aforementioned loss of probability from resolved to unresolved scales. Not even in the limit $N \rightarrow \infty$ can the unitarity of \mathcal{P} be restored: rather, the eigenfunctions tend to singular objects outside the Hilbert space, in tune with a continuous spectrum of \mathcal{P} .

The reader may have noticed that all eigenvalues in table I are real or almost imaginary. In fact, all eigenvalues we have identified as frozen inside the unit circle have phases corresponding to those of roots of unity, a fact demanding explanation. Clearly, since $\mathcal{P}^{(N)}$ is real the eigenvalues are either real or come in complex conjugate pairs, but no other phase than zero is distinguished by that argument. Again, the eigenfunctions offer further clues. We find that the phases of the complex eigenvalues are determined by the length p of the shortest periodic orbit present in an eigenfunction f as those of the p -th roots of unity. The following intuitive argument indicates that this is to be expected.

Assume an eigenfunction is mostly concentrated around a shortest unstable orbit with period p as well as a longer one with period p' . Denote by $\delta_{p,n}$ a “characteristic function” which is constant near the n -th point of the period- p orbit, $n = 1 \dots p$, and zero elsewhere. The truncated Frobenius-Perron operator $\mathcal{P}^{(N)}$ maps $\delta_{p,n}$ into $\mathcal{P}^{(N)}\delta_{p,n} = r_p\delta_{p,n+1}$ with the real positive factor r_p smaller than unity accounting for losses, in particular to unresolved scales. Independent linear combinations of the $\delta_{p,n}$ can be formed as $f_{pk} = \sum_{n=1}^p e^{i2\pi kn/p}\delta_{p,n}$ with $k = 1 \dots p$. Now consider a sum of two such functions, $g = f_{pk} + f_{p'k'}$, and apply $\mathcal{P}^{(N)}$. For g to qualify as an approximate eigenfunction we must obviously have $r_p \approx r_{p'}$ and $k/p = k'/p'$. But then indeed $\mathcal{P}^{(N)}g \approx r_p e^{i2\pi k/p}g$ and $[\mathcal{P}^{(N)}]^p g \approx r_p^p g$. The phase is thus dictated by the shortest orbit. Needless to say, the argument is identical to the one used before for the eigenfunctions living

in islands around elliptic orbits, save for $r_p = 1$ in those regular cases. Since orbits of low period are most likely to be resolved first, the eigenvalues found for $l_{max} = 40$ in table I have phases according to $p = 1, 2$ and 4.

Knowing which orbits are linked to a non-unimodular eigenvalue, we can adopt a cycle expansion to calculate decay rates from periodic orbits [11]. A cycle expansion of the spectral determinant, i.e. the characteristic polynomial of the Frobenius-Perron operator, allows for the calculation of resonances in hyperbolic system with high accuracy [12]. The spectral determinant is expressed in terms of the traces of the Frobenius-Perron operator $\text{Tr } \mathcal{P}^n$ as $d(z) = \prod_{n=1}^{\infty} \exp\left(-\frac{z^n}{n} \text{Tr } \mathcal{P}^n\right)$ and subsequently expanded as a finite polynomial up to some order n_{max} . Only the first n_{max} traces are required for the calculation of this polynomial. The traces $\text{Tr } \mathcal{P}^n$ are calculated by summing over hyperbolic periodic orbits of length n as $\text{Tr } \mathcal{P}^n = \sum \frac{1}{|\det(1-J)|}$ where the 2×2 matrix $J = \partial M^n(X)/\partial X$ is the linearized map M^n evaluated at any of the points of a contributing period- n orbit and $X = (\cos\theta, \varphi)$ the phase space point. The zeros of the polynomial which are insensitive against an increase of n_{max} are inverses of resonances.

The condition under which the ordinary cycle expansion of a spectral determinant converges is that all periodic orbits are hyperbolic and sufficiently unstable [2,11,12]. But if we only consider one ergodic region in phase space at a time, i.e. bar contributions from elliptic orbits, and impose a stability bound by including only the relatively few hyperbolic orbits identified in an eigenfunction of $\mathcal{P}^{(N)}$, we can still use the cycle expansion as follows. We assume the spectral determinant factorized as $d(z) = \prod_{i=1}^{\infty} d_i(z)$ with one factor d_i for the family of eigenfunctions to which a given set of periodic orbits contributes. Each such factor $d_i(z)$ is then calculated separately with the above well known expressions but restricting the periodic-orbit sum for the trace $\text{Tr } \mathcal{P}^n$ to the orbits previously identified as contributing to the eigenfunctions. In table II resonances reproduced via the spectral determinant from only few orbits show surprisingly good agreement with the resonance-eigenvalues of $\mathcal{P}^{(N)}$ for $\tau = 10$ and $l_{max} = 60$. The index n_{max} gives the order up to which the spectral determinant is expanded, i.e. the length of the longest (pseudo-)orbits employed. The total number of orbits used is given in brackets behind the resonances. For the resonance 0.8103 the three relevant orbits of period 1,2 and 4 are marked in the magnified region of the eigenfunction ($l_{max} = 60$) in figure 2c. The first repetition of the single period-2-orbit contributing to the resonance 0.6597 gives an almost diverging contribution to the spectral determinant, thus hindering its expansion to a higher order.

In the cycle expansion the phases of the resonances are reproduced exactly since they are again directly determined by lengths of orbits. If p is the shortest orbit

length used in $d_i(z)$, the polynomial can as well be written as a polynomial in z^p thus allowing the zeros to have the phases of the p th roots of unity.

As a final check on the physical meaning of our frozen eigenvalues with moduli smaller than unity as Frobenius-Perron resonances we have compared these moduli with rates of correlation decay. In a numerical experiment we investigated the decay of the correlator $C(n) = [\langle \rho(n)\rho(0) \rangle - \langle \rho(\infty)\rho(0) \rangle] \cdot [\langle \rho(0)\rho(0) \rangle - \langle \rho(\infty)\rho(0) \rangle]^{-1}$. Depending on the choice of $\rho(0)$ different long-time decays are observable. We chose $\rho(0)$ as covering the regions where the hyperbolic orbits relevant for a given resonance are situated. Figure 1c illustrates the very good agreement between the long-time decay of $C(n)$ (dots) and the decay as predicted by the corresponding resonance 0.81 (full line). Together with the resonances at $l_{max} = 60$ table II displays the associated decay factors by which $C(n)$ decreases over one timestep, obtained from a numerical fit. Again the agreement is convincing.

In conclusion, we have presented a method to determine Frobenius-Perron resonances and the associated phase-space structures, applicable to systems with mixed phase spaces. The acquired knowledge of phase space structures allows to check the accuracy to which resonances are determined by the otherwise independent approaches of cycle expansion and correlation decay.

We are grateful to Shmuel Fishman for discussions initiating as well as accompanying this work. Support by the Sonderforschungsbereich "Unordnung und große Fluktuationen" and by the grant GAAV No. A1048804 of the Czech Academy of Sciences is thankfully acknowledged. F. H. also thanks the Isaac Newton Institute for hospitality during the workshop "Supersymmetry and Trace Formulae" in 1997 during which this work was begun; especially fruitful interactions with Ilya Goldscheid were made possible there.

-
- [1] D. Ruelle, Phys. Rev. Lett. **56**, 405 (1986)
 - [2] D. Ruelle, J. Stat. Phys. **44**, 281 (1986)
 - [3] M. Pollicott, Invent. Math. **81**, 415 (1985)
 - [4] V. Baladi, J.-P. Eckmann, and D. Ruelle, Nonlinearity **2**, 119 (1989)
 - [5] A. V. Andreev and B. L. Altshuler, Phys. Rev. Lett. **75**, 902 (1995); O. Agam, B. L. Altshuler, and A. V. Andreev, Phys. Rev. Lett. **75**, 4389 (1995); A. V. Andreev, O. Agam, B. D. Simons, and B. L. Altshuler, Phys. Rev. Lett., **76**, 1 (1996); A. V. Andreev, B. D. Simons, O. Agam, and B. L. Altshuler, Nuclear Physics B, **482**, 536 (1996).
 - [6] M. R. Zirnbauer in: I.V. Lerner, J.P. Keating, and D.E. Khmelnitskii (eds.), *Supersymmetry and Trace Formulae: Chaos and Disorder* (Kluwer Academic, New York, 1999)

- [7] K.Pance, W. Lu, S. Sridhar, arXiv:nlin.CD/0004006
- [8] S. Fishman in: I.V. Lerner, J.P. Keating, and D.E. Khmelnitskii (eds.), *Supersymmetry and Trace Formulae: Chaos and Disorder* (Kluwer Academic, New York, 1999)
- [9] M. Khodas and S. Fishman, Phys. Rev. Lett. **84**, 2837 (2000)
- [10] M. Khodas and S. Fishman, chao-dyn/9910040 (1999)
- [11] P. Cvitanović et al., *Classical and Quantum Chaos: A Cyclist Treatise*, (Nils Bohr Institute, Copenhagen, 1999) (www.nbi.dk/ChaosBook/)
- [12] F. Christiansen, G. Paladin, and H. H. Rugh, Phys. Rev. Lett. **65**, 2087 (1990)
- [13] E. C. Titchmarsh, Proc. Roy. Soc. London Ser. A **210**, 30 (1951)
- [14] M. Reed and B. Simon, *Methods of Modern Mathematical Physics IV: Analysis of Operators* (Academic Press, New York, 1978).

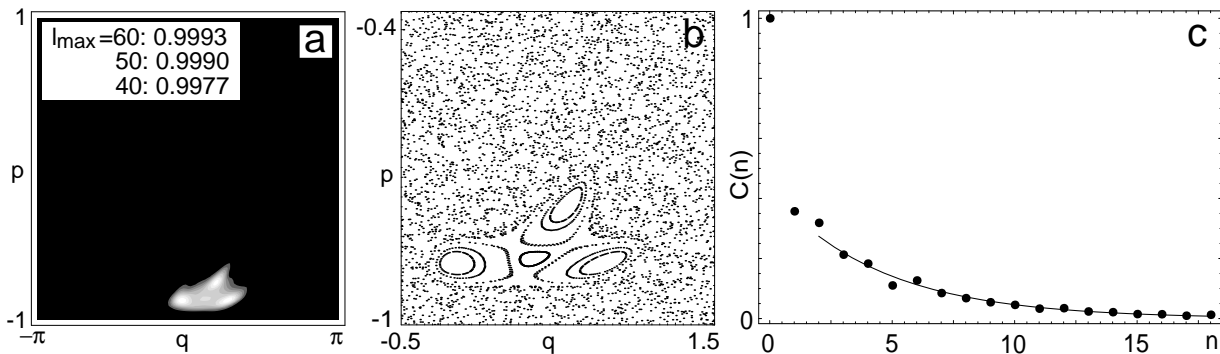


FIG. 1. (a) The eigenfunction to the almost unimodular eigenvalue 0.9993 for $\tau = 4$, $l_{max} = 60$ is sharply localized on elliptic islands surrounding a period-3-orbit in phase space. (b) Phase space portrait of the elliptic islands supporting the eigenfunction. (c) The decay of the correlator $C(n)$ (dots) [with the initial density localized in the region shown in figure 2c] and the decay predicted by the corresponding resonance 0.8103 (full line) agree well (see also table II).

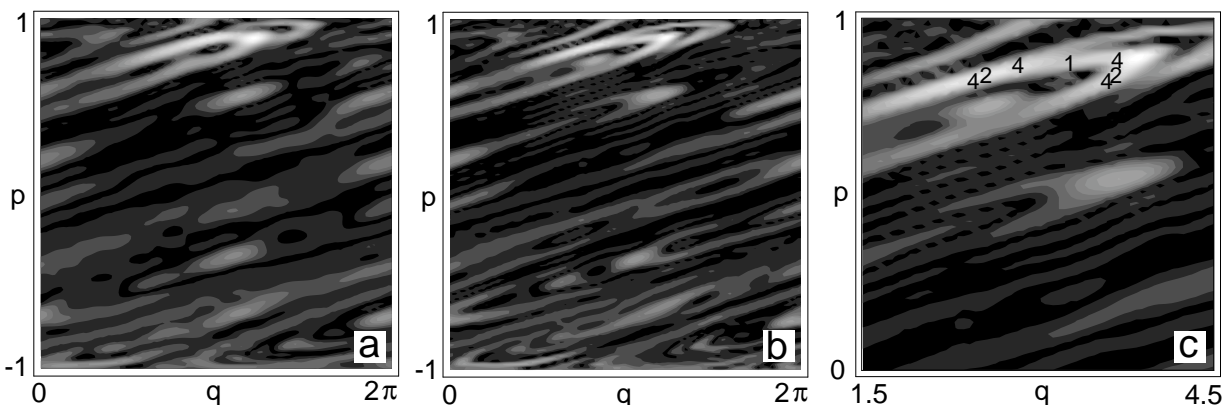


FIG. 2. Eigenfunction to the resonance-eigenvalue 0.81 for $\tau = 10$ and (a) $l_{max} = 40$, (b) $l_{max} = 60$. While the coarse structures are identical, finer structures appear in the eigenfunction with the higher resolution. (c) Magnification of the region of large amplitude in figure 2b. The numbers indicate the positions of the three periodic orbits of lengths 1, 2 and 4 which are used in the cycle expansion up to order $n_{max} = 4$.

$l_{max} = 40$	$l_{max} = 50$	$l_{max} = 60$	$l_{max} = 70$
0.8116	0.8205	0.8103	0.8076
0.7457	0.7547	0.7470	0.7459
-0.7432	-0.7475	-0.7510	-0.7465
-0.0063	-0.0123	-0.0079	-0.0042
$\pm i 0.7431$	$\pm i 0.7515$	$\pm i 0.7517$	$\pm i 0.7414$
-0.6443	-0.6188	-0.6377	-0.6347

TABLE I. Resonances appearing for $\tau = 10$ at $l_{max} = 40, 50, 60$ and 70 .

$l_{max} = 60$	0.8103	-0.7510	0.6597
$n_{max} = 1$	0.2185{1}	-	-
$n_{max} = 2$	0.7070{2}	-	0.4969{1}
$n_{max} = 4$	0.7664{3}	-0.7483{4}	-
decay of $C(n)$	0.8005	0.7697	0.6783

TABLE II. First row: resonances obtained from the truncated propagator for $\tau = 10$ and $l_{max} = 60$. Below: corresponding results from cycle expansion up to order n_{max} . The total number of primitive orbits employed is given in curly brackets. Last row: associated decay factors by which $C(n)$ decreases over one timestep, obtained from numerical fit.